The Expanse: Advnaces in Design, Optimization, and Simulation of Pantographic Structures

Mitchell Bennett Fogelson

CMU-ME-00-00

June 2025

College of Engineering
Mechanical Engineering Department
Carnegie Mellon University
Pittsburgh, Pennsylvania

Thesis Committee
Zachary Manchester, Chair
Jonathan Cagan
Minchen Li
Jeffrey I. Lipton (*Northeastern University*)

Submitted in partial fulfillment of the requirements for the degree of Doctor of Philosophy.

Keywords: linkage design, co-design, differentiable physics, generative ai, state-estimation, deployable structures, space deployables

TODO

Abstract

The capabilities of our robotic systems are mostly being thought as limitations of control algorithms, compute power, and complex models. Robot designs have all but converged on the serial chain solutions, which are easy to design, optimize fixed continuous parameters and conform to the existing simulation frameworks. However these solutions are failing to understand the influence and trade-off between more complex designs whose geometry, composition, and compliance enable behaviors without the need for complex control, models or compute. In the aerospace community these designs have been essential to achieve the successful missions of systems like James Webb and many more. However, the systems require lots of physical testing and analysis to ensure success. In this work we imporve the capabilities of pantographic designs, reduce the design burden with new optimization methods, and introduce a differentiable simulation that supports these design for analysis and control. This thesis advances the capabilities of mechanical systems for robotic and aerospace solutions for future missions and goals.

Acknowledgments

TODO

Contents

List of Figures

List of Tables

List of Algorithms

Chapter 1

Introduction

This dissertation introduces ... TODO [15]

In the period between ... TODO

1.1 Summary of publications

Chapter 2

Background

This chapter provides a thorough description of ... TODO

2.1 Pantographic Structures

2.2 Reinforcement Learning

2.3 Mixed Integer Optimization

2.4 Differentiable Simulation

2.5 State Estimation

2.6 System Identification

Chapter 3

Non-Planar Hierarchical Composition of Extending Metamaterials for Deployable Load-Bearing Structures

Structures and materials with geometric hierarchy exhibit enhanced strength-to-weight ratio. In volume-constrained scenarios, such as packing payloads into a rocket fairing, deployable structures enable the efficient transport of load-bearing forms. When optimizing the strength-to-packing efficiency of payloads, this work shows that non-planar hierarchical compositions of deployable structures can dramatically improve performance. To this end, the paper describes a new pantographic design, the Pop-Up Extending Truss (PET), which uses the composition of scissor elements to enable out of plane reorientation, enhancing the bending stiffness by over 100% compared to other translational scissor variants with equal mass and linear packing. Additionally, by composing multiple PET structures in a Kresling pattern we show this new structure - which is refered to as HERDS (Hierarchical Extending and Reorienting Deployable Structures) - is capable of supporting 10x higher bending, compressive, torsional, and tensile stiffness at 25-200x extension ratios compared to non-hierarchical deployable structures when designs are constrained by initial volume. A physical HERDS prototype achieved a 50x extension ratio and supported compressive and bending loading. Practical applications for this new class of deployable structures include large space structures, deployable infrastructure, and compact medical devices.

3.1 Introduction

Engineers continue to push the boundaries of large-scale space structures to extend the capabilities outside of earth. One such example of this is the James Webb Space Telescope, with its sun shield spanning over 10 tennis courts, enabling the capture of unprecedented images of the universe. Previous work by the authors proposed a preliminary evaluation of a kilometer-scale space structure from a single rocket launch to support artificial gravity [15]. A kilometer-scale design is 50x longer than the JWST and 10x longer than the

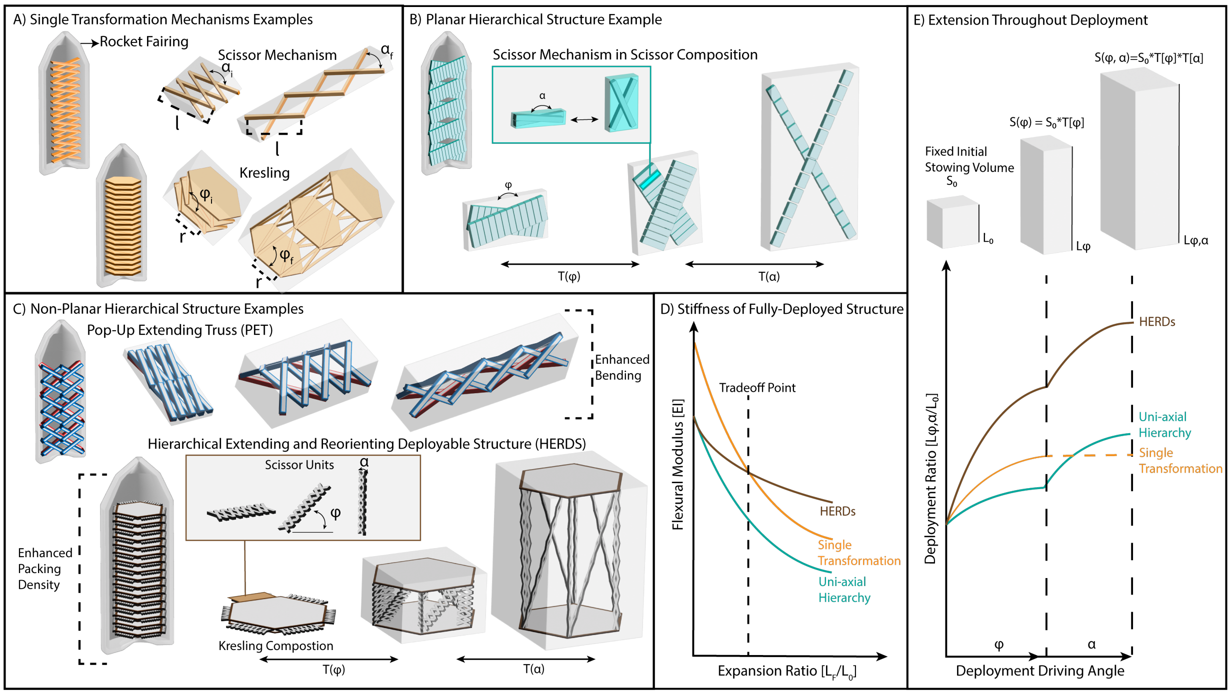

Figure 3.1: This figure illustrates various mechanical design concepts for structures that can extend: **A) Single Transformation Mechanisms:** shows a scissor mechanism representing a structure that leverages folding and a Kresling origami structure that leverages wrapping transformation. **B) Hierarchical Deployment (Same Axis Transformation):** demonstrates a two-step transformation along the same axis showing a large area change, but not a useful hierarchy for extension applications. **C) Hierarchical Deployment (Multi-Axis Transformation):** depicts a multi-axis transformation where the structure goes through a hierarchical expansion that supports extension through both deployment transformations. **D) Graph of Bending Stiffness vs. Expansion Ratio:** shows the relationship between bending stiffness and the expansion ratio, highlighting a trade-off point. It compares different design strategies: HERDs (hierarchical expansion of reorienting designs), single transformation mechanisms, and uni-axial hierarchy. **E) Expansion Given Constant Beam Width:** visualizes the volume expansion $V0$ from an initial compact state $L0$ through the transformations $T(a)$ and $T(b)$ to reach a final expanded state $L(a, B)$, while maintaining a constant beam width.

current ISS. The design of such a structure must optimize strength-to-packaging efficiency to achieve this in a single launch with existing space vehicles. Alternative approaches aim to replicate Earth-based construction methods by transporting raw materials and assembling structures in space [50]. However, this requires advanced coordinated robotic systems, which is an area of ongoing research. More commonly, as seen with JWST, a collapsible structure is prefabricated on Earth and compactly stowed for a launch with no in-space assembly required. This work builds on the previous study by the authors [15] by performing a more extensive design sweep of the non-planar hierarchical deployable mechanism and its subcomponents, offering a deeper analysis of design parameters, trade-offs, and metamaterial behavior in PET and HERDS structures.

The aerospace and architecture industry has led advances in single-transforming load-bearing mechanisms as described in [13]. The aerospace community, constrained by rocket fairing size has demonstrated many examples of booms [8, 14, 28, 54, 52, 51, 48, 42, 36] and masts [3, 19, 27, 33, 45, 53, 55]. Although past successes have demonstrated the viability of these approaches, continued innovation remains crucial for future missions.

In the literature, many extending space structures exist, which have been segmented by Wang et al. [47], in a review paper on deployable space structures, into inflatable, elastic, and pantographic solutions. All of these structure types have a place in the space infrastructure landscape, and no one solution is a silver bullet for current and future deployable structure problems.

Inflatable deployable mechanisms offer several advantages over rigid structures, particularly in terms of weight reduction and high packaging efficiency. In the review paper by Wang et al. [47], they include the following successful examples of inflatable deployable structures include the inflatable antenna used in the Echo I mission [18], the antenna deployed on the STS-123 Space Shuttle Endeavor [9], the inflatable radar (SAR) for Earth-sensing missions [29], and the inflatable solar arrays used on the Mars Rover [4]. However, several technical challenges remain, including optimizing packing strategies [38], understanding inflation dynamics [10], and developing accurate models [12]. For kilometer-scale space structures intended for artificial gravity, inflatable systems are less suitable due to their susceptibility to micrometeoroid impacts and vulnerability to global buckling failure.

The use of thin-walled elastic members is touted for their high strength-to-weight properties and simple construction [14, 52, 36]. Variations of such structures display extension ratios exceeding 300x, but rely on material elasticity to deploy and maintain their structure [36]. Practical examples of these systems are the iROSA structures on the ISS [40] and DaGHR antenna [22]. Although these structures offer advantages in self-deployment, the release of stored strain energy is often unpredictable, difficult to control, and highly dynamic. This can lead to unwanted vibrations and potential secondary damage. Thin-walled composite structures also suffer from low impact resistance, presenting durability challenges in space environments [28]. Additionally, these structures face scaling limitations due to the significant elastic energy stored during deployment and their lower structural rigidity compared to conventional truss systems, making them less viable for kilometer-scale applications in microgravity.

Deployable truss structures, also known as pantographic structures, offer design versatility, allowing for customization and adaptation to various configurations based on specific deployment requirements. Compared to telescopic structures, they provide a higher spatial packaging efficiency and reduced weight. However, their design and deployment mechanisms are inherently complex and often require a large number of parts. In addition, Pantagraphic structures are limited by the aspect ratio or material thickness to achieve higher extension ratios. For a scissor-based mechanism, that means that the individual truss elements become very long and thin, leading to the possibility of local buckling. In the review paper by Wang et al. [47], they highlight the following deployable truss structures have been implemented in various applications, including extension masts [24, 45, 34, 23, 35], extension arms [7], flexible solar array paddles [25], and telescopic masts for NASA's Shuttle Radar Topography Mission [46]. Parallel deployable truss structures have been utilized in planar solar arrays, such as those on the Chinese Dongfanghong (DFH)-4 [56] and DFH-5 [30] satellites, the Spacebus Earth communication satellite [44], and the Shijian 20 satellite [11]. Another common application is for parabolic antennas, including those on the ETS-VIII [31] and Environment-1C [41] satellites, as well as in MegaFlex solar arrays [58]. These applications benefit from pantographic structures, which are inherently free of strain energy, material-agnostic, and scalable, making them well-suited for large deployable systems. To the authors' knowledge, no kilometer-scale deployable truss structure has been deployed.

	Inflatables	Elastic	Pantographic	**Non-Planar Hierarchical Pantographs (Ours)**
Controlability	×	×	✓	✓
Retractability	×	✓	✓	✓
Scalability	✓	×	✓	✓
Redundancy	×	×	✓	✓
High Strength to Packing Ratio	✓	✓	×	✓

Table 3.1: Comparison of deployable structure classes including Inflatables, Elastic Structures, Pantographic, and our proposed Hierarchical Pantographic Structures. Hierarchical Pantographs enhance key advantages such as retractability, scalability, and strength-to-packing ratio while maintaining the benefits of redundancy and control.

This work looks at a rocket fairing packing problem, where the structure seeks to both maximize the usable volume in the fairing in the stowed state and the linear extension in the deployed state. At this scale, elastic deployable solutions are not feasible due to the large shear stress in the stowed state. Additionally, inflatable structures are not considered due to their limitations for bending applications. When constrained by a predetermined initial volume, Pantagraphic deployable structures must minimize material thickness to enhance packing density to achieve the necessary extension ratios. This necessity introduces an inherent compromise between the extent of extension achievable and the structure's load-bearing capacity. The geometric hierarchy in natural and architected structures improves the strength-to-density ratio for improved efficiency and performance [26, 37, 2, 39].

Biology incorporates structural hierarchy in their additive building processes, enabling enhanced mechanical properties [16]. Bird bones exhibit structure on multiple length scales to match necessary loading requirements at extremely low weight [43]. Wood and plant stems use structural hierarchy to provide mechanical support against the elements [26, 5]. In engineered systems, this hierarchy is incorporated in large structures, such as radio towers, bridges, and quite famously, the Eiffel tower [26]. These structures are referred to as space frame structures and credited to Alexander Graham Bell in 1903 [6]. With digital fabrication, hierarchical mechanical metamaterials can be tuned to exhibit extremal properties [1, 2]. Despite the structural utility of hierarchy, the benefits of hierarchical designs of transforming and deployable structures have been muted. We define "deployable hierarchy" as the combination of multiple transforming mechanisms arranged at different size scales, which has not been demonstrated in non-planar cases. Planar hierarchy has demonstrated synchronized deformations and auxetic properties [49, 17], with applications for architected area changes, but no added structural benefit over traditional extending structures (Figure **??**.B).

Our research introduces a novel class of mechanical metamaterial structures that leverage non-planar deployable hierarchy to combine multiple separate deployable mechanisms at different size scales to improve the tradeoff between extension and strength-to-weight ratios with a wide range of tunable properties. This work makes the following contributions:

1. We demonstrate that the non-planar deployable hierarchical composition of extension mechanisms enhances material packing density, improving mechanical properties at high extension ratios.
2. By applying this framework to scissor mechanisms, we introduce the Pop-Up Extending Truss (PET) mechanism, which offers better packing density and bending properties than existing scissor-like variants.
3. We provide an example of Hierarchical Extending and Reorienting Deployable Structures (HERDS), a non-planar deployable hierarchical structure that integrates the PET and Kresling mechanisms. Finite element simulations demonstrate improved mechanical properties at high extension ratios, and a prototype implementation of the structure is presented as a path toward practical applications.

3.2 Results

3.2.1 Hierarchical Composition of Deployables for High Extension

Composition of Linear Extension Deployables in Kresling Pattern

Through sliding, wrapping, or pivoting their material, structures can stow and expand, manipulating the pose of material members and thus volume. This work looks at structures that extend to many times their stowed length. When fully deployed, these structures can have high length-to-width ratios, making them vulnerable to bending and buckling.

Therefore, the structure's extension ratio (ER) – the ratio of the final length to the stowed length – and flexural modulus (EI) – a metric used to evaluate bending stiffness measured in the deployed state – are considered to assess a structure for load-bearing applications [32]. Without a loss of generality, this work focuses on 1-DOF extending mechanisms, where a single parameter, such as the angle between the scissors, can represent the state of the structure. A structure seeking to achieve a high extension ratio must maximize the packing density by pivoting, sliding, or wrapping the subcomponents in relation to one another. The volume of a pivoting 1-DOF mechanism, such as a scissor mechanism or mechanical Kresling, described in Zhai et al. [57], can be seen in Figure **??**.A, transforms based on the rotation of the internal beams. The extension ratio for a translational scissor is expressed by:

$$ER_{scissor} = \frac{l * cos(\alpha_f)}{l * cos(\alpha_i)} \approx \frac{l}{t} \quad \text{when} \quad cos(\alpha_f) \approx 1 \;\; \& \;\; n >> 1 \tag{3.1}$$

where α_i, α_f are the initial and final angles of the scissor, l is the link length of the scissor, t is the thickness of the link, and n is the number of scissor units connected together. The extension ratio of the scissor mechanism is the ratio of the cosine of the final angle between the members to the initial angle of the members. This extension ratio of a scissor can be approximated as the aspect ratio of an individual member when there are many scissor units combined. The extension ratio of a Kresling mechanism is:

$$ER_{Kresling} = \frac{r\sqrt{(2 * cos(\phi_f) - 1)}}{r\sqrt{(2 * cos(\phi_i) - 1)}} \approx \frac{r}{2t} \quad \text{when} \quad \frac{t}{r} << 1 \tag{3.2}$$

where r is the radius of the mechanism, ϕ_i, ϕ_f is the angle offset between the top and bottom plates of the Kresling (twist), and t is the thickness of the Kresling members. Here, the extension ratio is again a ratio of the final angle to the initial angle and can also be approximated as an aspect ratio of the kresling members, which is a function of its radius.

This shows that the only way to achieve high extension ratios for these mechanisms is to have high aspect ratio elements that are prone to local buckling when subjected to bending loads. Similarly, for other 1-DOF mechanisms that use pivoting and sliding deployment, these designs only contain a single packing direction. This means that the magnitude of possible expansion is fully determined by the dimensions of the initial bounding volume and the thickness of the individual members making up the mechanism **??**.A. This problem is exacerbated in the practical design of deployable mechanisms when the original bounding dimensions are constrained, leading to thinner individual members, leaving designs susceptible to buckling and local deformation.

Non-planar deployable hierarchy can be used to increase the extension ratio while maintaining favorable member aspect ratios. One example highlighted in this paper is the composition of scissor elements and the Kresling pattern, Figure **??**.C. This new structure hierarchically extends through multiple sequential reorientations of the individual elements. This hierarchical composition enables tighter packing of the sub-mechanisms to achieve high extension ratios. The extension ratio from HERDS is approximately as follows:

$$ER_{HERDS} = \frac{n * l * cos(\alpha_f)}{r\sqrt{(2 * cos(\phi_i) - 1)}} \approx \frac{n * l}{2t} \approx \frac{r * l}{2t^2} \quad \text{when} \quad cos(\alpha_f) \approx 1 \;\; \& \;\; \frac{t}{r} << 1 \quad (3.3)$$

where α_f is the angle of the scissor mechanism, ϕ_i is the twist angle of the Kresling, t is the thickness of the scissor links, n is the number of scissor units, l is the length of the scissor links and r is the radius of the Kresling. The hierarchical composition increases the tunable parameters to achieve high extension, including the number of scissor units, kresling deployment angle, kresling radius, and member aspect ratio.

An important note about the proposed design from Figure ??.C, the hierarchical composition of the mechanism transformations must occur sequentially. The Kresling transformation, $T[\phi]$, is performed first, reorienting the scissor mechanism. Then, the scissor mechanism's transformation, $T[\alpha]$, can deploy the subcomponents smoothly, increasing the system extension. These transformations are not commutable; for example, in the collapsed state, the transformation of the scissor mechanism, $T[\alpha]$, would not lead to the effective extension of the mechanism. This is not always the case when composing deployable mechanisms, as in Figure ??.B, the transformations commute.

By manipulating the orientation of substructure stacking through deployable hierarchical design, we achieve high packing efficiency without increasing the component aspect ratio. This demonstrates the benefits of hierarchical deployable structures for extension ratio but does not consider the structure's stiffness yet. The stiffness of the deployed structure depends on the extended material's final deployed architecture. The next section considers various scissor structures and their effect on hierarchical design stiffness.

3.2.2 Pop-Up Extending Truss: A Non-Planar Composition of Scissor Elements

A translational scissor mechanism has a low flexural modulus when fully deployed, making it susceptible to bending failures. Using a translational scissor mechanism as the substructure for the HERDS leads to a major limitation of the overall mechanical stiffness. Through finite element analysis, the flexural modulus (bending stiffness) of the scissor mechanism is shown to be less than that of a solid beam with the same cross-sectional area, as seen in Figure ??.A. While the hierarchical composition of a scissor and Kresling mechanism provides extension benefits, the poor bending stiffness limits the usefulness of the hierarchical design.

3.2.3 Improved Bending Stiffness

By applying a non-planar composition of scissor mechanisms, we developed a novel deployable structure known as the Pop-Up Extending Truss (PET), first described by Fogelson et al. in [15]. The PET consists of three scissor mechanisms: two short-link translational units and one long-link translational unit with a polar offset. This offset enables out-of-plane motion during deployment, resulting in multi-axis reorientation of the substructures. This

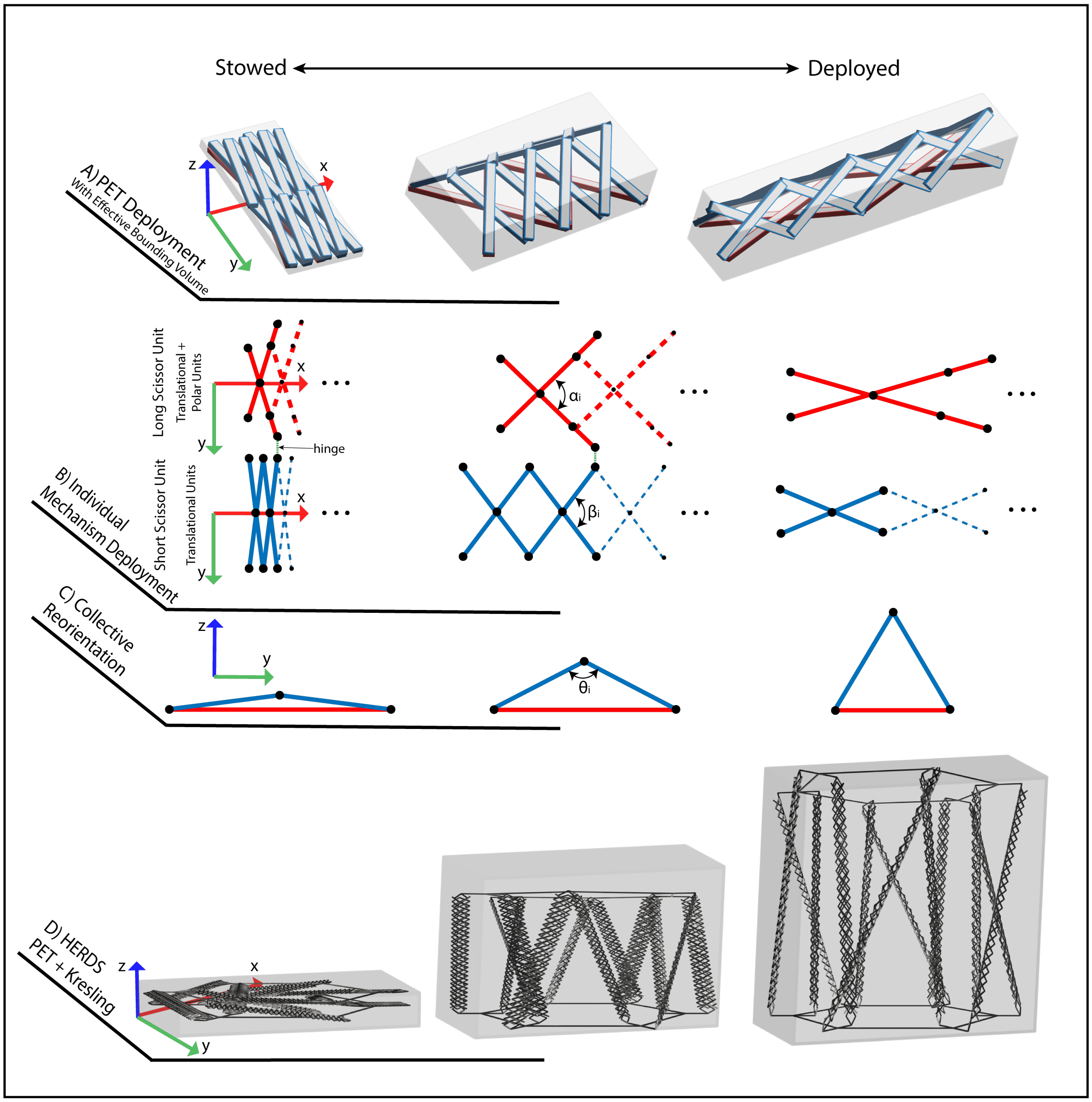

Figure 3.2: This figure presents the Pop-Up Extending Truss (PET) structure, a novel scissor-like mechanism , and a HERDS mechanism that consists of 12 PET structures in a Kresling pattern to achieve the non-planar deployable hierarchy. **A) PET Deployment:** provides an isometric perspective of the PET, comprising three interconnected scissor elements: the blue ones are Short-Link Scissor Members (SLSM), while the red one is the Long-Link Scissor Member (LLSM). The design facilitates a compact arrangement by allowing the SLSMs to collapse onto the LLSM. Upon deployment, the SLSMs extend into a triangular truss configuration, thereby improving the structure's resistance to bending. **B) Individual Mechanism Deployment:** showcases a solitary scissor element, depicting the PET's top view and the pivotal state parameter alpha as it moves from a stowed to an extended state. **C) Collective Reorientation:** presents the PET's frontal view, illustrating the transition of the SLSMs from a flat, packed condition in the stowed phase to an elevated, triangular form upon deployment. **D) HERDS (PET + Kresling):** presents a rendering of a HERDS mechanism composed on 12 PET structures in a Kresling pattern through the deployment with the effective boundary.

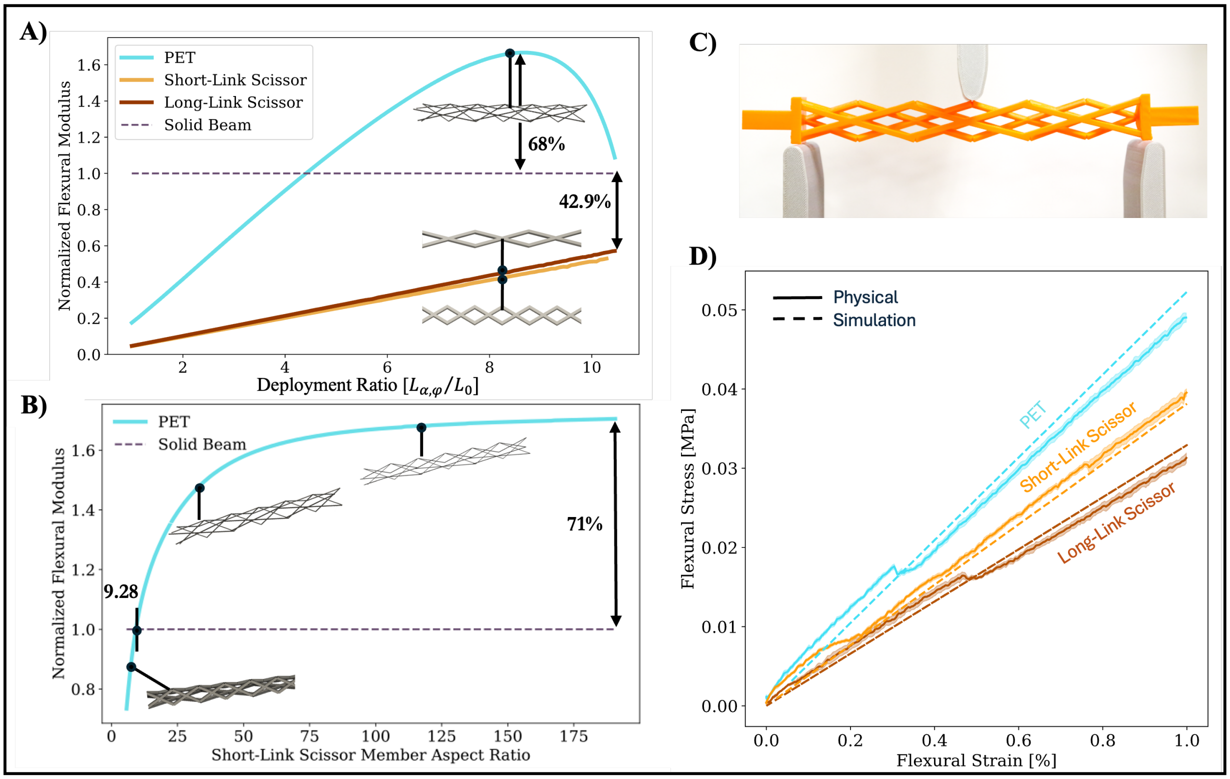

Figure 3.3: This figure evaluates the performance characteristics of the Pop-Up Extending Truss (PET) against traditional solid and scissor-type beams through both theoretical and empirical analyses: **A) Flexural Modulus vs. Scissor Deployment:** Demonstrates that as the PET deploys, maintaining a given member aspect ratio, it consistently outperforms basic scissor structures in flexural modulus. However, these scissor variants do not achieve a higher utility than a solid beam within the depicted extension ratio range, showing a 42.9% reduction in normalized flexural modulus for the solid beam. **B) Flexural Modulus vs. Link Aspect Ratio:** Illustrates the threshold at which the PET's short-link scissor member's aspect ratio surpasses the utility of a conventional solid beam, indicating a 71% increase in normalized flexural modulus.**C) Physical Testing:** Depicts the physical test units used in an Instron machine, which were instrumental in validating and calibrating the simulation models developed in ANSYS.**D) Physical Testing vs. Simulation:** Confirms the alignment between the beam model approximations and the physical testing results, showing a close correlation between the observed physical and the simulated flexural stress across a range of flexural strains for the PET, short-link scissor and long-link scissor beams.

unique composition allows the structure to simultaneously extend and expand, forming a triangular truss configuration (Figure **??**). The PET differs from other triangular scissor mechanisms, such as [53], which retain a triangular void in the center when collapsed. In contrast, the PET structure flat-packs, significantly improving packaging density and making it well-suited for integration into a non-planar deployable hierarchy following a Kresling pattern.

In the stowed state, the long scissor unit occupies the width of the two smaller units, enabling flat packing. As the PET deploys, the width of the long scissors changes at a different rate than that of the short scissors, which forces an out-of-plane reorientation and results in the formation of a triangular truss. This geometric transformation increases the structure's minimum bending moment of inertia, thereby enhancing its resistance to bending and buckling.

For this analysis, all structures were modeled using beam-based finite element methods (FEM) to evaluate comparative structural performance. The material type and Young's modulus (E) were held constant, so differences in stiffness are primarily due to changes in the bending moment of inertia, $I_x = \int_A y^2 dA$ or $I_y = \int_A x^2 dA$. In idealized systems, placing structural mass further from the centroid increases bending and buckling resistance. However, in truss and lattice-based structures, both local and global deformation modes must be considered as the aspect ratios and densities of constituent beams change. To evaluate performance, we conducted a simulated cantilever beam test across various extending topologies—independent scissor mechanisms, the PET, and a solid reference beam with equivalent bundled cross-sectional area—under the weakest configuration: in-plane bending with a fixed displacement. Flexural modulus was estimated using:

$$EI = \frac{FL^3}{3d} \tag{3.4}$$

where F is the reaction force, L is the effective length of the mechanism, and d is the tip displacement.

Figure **??**.A shows that as the PET extends, its effective flexural modulus increases at a greater rate than either of the short- or long-link scissor mechanisms alone, with a maximum observed improvement of 68% over a solid beam with equivalent bundled cross-sectional area. We additionally compare the PET to independent short- and long-link scissor mechanisms adjusted to have equal mass by increasing their cross-sectional area. The PET, when built from square-cross-section beams, achieves a 50% stowing advantage over an equivalent-mass scissor mechanism with rectangular cross-section. Structurally, the PET demonstrates a 111% bending stiffness improvement over the long-link scissor and a 115% improvement over the short-link scissor.

To validate the accuracy of the beam model approximation used in the FEA simulation, we conducted physical tests using an Instron machine, as shown in Figure **??**.C. The correlation between the experimental results and the simulated structures is illustrated in Figure **??**.D. Additional information about the Sim2Real validation and parameters can be found in SM Section 5.

Scaling Effects of PETS

To understand the PET design space tradeoffs, Figure **??**.B compares the PET flexural modulus of various member aspect ratios to a square cross-sectional beam of equal area. At low aspect ratios (shorter/thicker members), the mass of the PET remained close to the centroid, offering no significant moment of inertia benefit while simultaneously having sparse connectivity. As a result, the solid beam outperformed the PET. As PET member aspect ratios increased, the material was distributed farther from the centroid, causing the effective bending moment of inertia to increase. When the minimal aspect ratio of the PET surpassed 9.28, we saw improved flexural modulus results compared to those of the solid beam. As the PET member aspect ratio continued to increase, local bending of the slender beams became the dominant deformation mode, and the PET flexural modulus asymptotically approached 71% improvement over the solid beam.

The PET's aspect ratio directly correlates to the extension ratio (ER) and bending stiffness. By mass, hierarchical deployable structures with PETs as subcomponents only become structurally beneficial when the PET supports higher extension ratios. Many applications for deployable structures are volume rather than mass-constrained, making packing density an important consideration along with relative flexural modulus. The bespoke design enables the members to attain a stowage density of 50% greater by reducing the height in the direction orthogonal to expansion, as opposed to a scissor mechanism with the same extension ratio and mass. This stowing benefit does not directly boost the ER of the PET, but within HERDS, the increased stowed density aligns with the extension axis.

3.2.4 Design Tradeoffs of Non-Planar Hierarchical Deployable Mechanisms

In this section, we revisit the volume-constrained design problem introduced in Section **??**, focusing on the creation of kilometer-scale deployable structures from a single launch, Figure **??**.A. We conduct a global design space sweep comparing the performance of the proposed non-planar hierarchical mechanism (HERDS) with its constituent substructures: the PET and Kresling (KRES) mechanisms. To systematically evaluate these structures, we generated over 2,300 designs—approximately 500 HERDS, 1,000 PETs, and 800 KRES—by sweeping key geometric parameters including member thickness and deployment angle, Figure **??**.B. These parameters were selected for their direct impact on stowed and deployed height, allowing us to sample designs across a wide range of extension ratios (5x–200x).

All designs were simulated using Finite Element Analysis (FEA) in ANSYS®APDL[20], accessed through its Python API [21]. The structures were modeled using BEAM188 elements with fixed joints (excluding joint mass) and subjected to bending, tension, compression, and torsional loading. For bending, compression, and tension simulations, we applied a displacement equal to 1% of the final structure length, while torsional analysis used a fixed angular displacement of 3.6°. A full description of model assumptions, material properties, boundary conditions, and solver settings is included in SM Section 5.3, 5.4, 6, SM Figure 8-9, and SM Table 2-3.

To contextualize performance across varying sizes and topologies, all results were normalized using the average performance of the HERDS designs. This allows for a clear comparison of stiffness trends across different structures and extension ratios. Only designs with extension ratios greater than or equal to 77x meet the kilometer-scale deployment target, however, we report results across the entire sampled range (5x–200x) to identify the threshold at which HERDS surpasses its substructures. Data corresponding to extension ratios below 77x is shaded in grey in Figures **??**.C–F.

The results of this study reveal that hierarchical structures (HERDS) consistently outperform PET and KRES mechanisms in all loading conditions—bending, compression, tension, and torsion—once the extension ratio exceeds approximately 25x. Figure **??**.C–F plots normalized stiffness as a function of extension ratio for each loading mode. As expected, stiffness generally decreases with increasing extension ratio across all structures. However, the rate of decline varies significantly.

KRES designs exhibit relatively high stiffness in bending, compression, and tension at low extension ratios but degrade sharply beyond 25x, often failing to converge due to local buckling instabilities. Furthermore, KRES designs perform the worst under torsional loading across all extension ratios, likely due to their unidirectional rotational compliance.

PET designs, on the other hand, demonstrate excellent deployment stability up to a 200x extension ratio without local buckling, particularly excelling in torsional stiffness. However, PETs show weaker bending, compression, and tension stiffness at low-to-moderate extension ratios when compared to KRES. This performance gap is likely due to the underutilization of available fairing volume, as PETs only occupy a small portion of the 5-meter diameter constraint.

HERDS structures strike a compelling balance between deployability and structural integrity. Beyond 25x extension, they consistently outperform both PET and KRES structures in all loading conditions. Importantly, these trends persist even after normalizing by mass, as shown in Figure SM 9 in the supplementary materials. However, we note that hierarchy is not always beneficial: below 25x extension, simpler substructures may offer better performance. Still, across the full design sweep, hierarchical composition reduces stiffness degradation at high extension ratios, validating the mechanical advantages of the HERDS approach.

To further explore these findings, we fabricated and tested a physical HERDS prototype, as described in the following section, to assess practical implementation and deployment reliability.

3.2.5 Fabrication and Testing of Prototype

We constructed a practical scaled demonstration of the HERDS that integrates PETs and Kresling deployable mechanisms. The prototype was fabricated from over 1500 3D printed components and acrylic plates, combined to make 2 hierarchical Kresling cells, each with outer sub-members made of PETs. The structure smoothly transitioned from a height of 2.5 inches (0.05m) to approximately 8 feet (2.54m), using gravity as the deployment force (Video 1). Figure **??**.A demonstrates the structure deployment, starting with the flat-packed configuration and extending to the full-length truss. Individual PET beams extended and popped into triangular trusses, with flexible TPU joints connecting individual

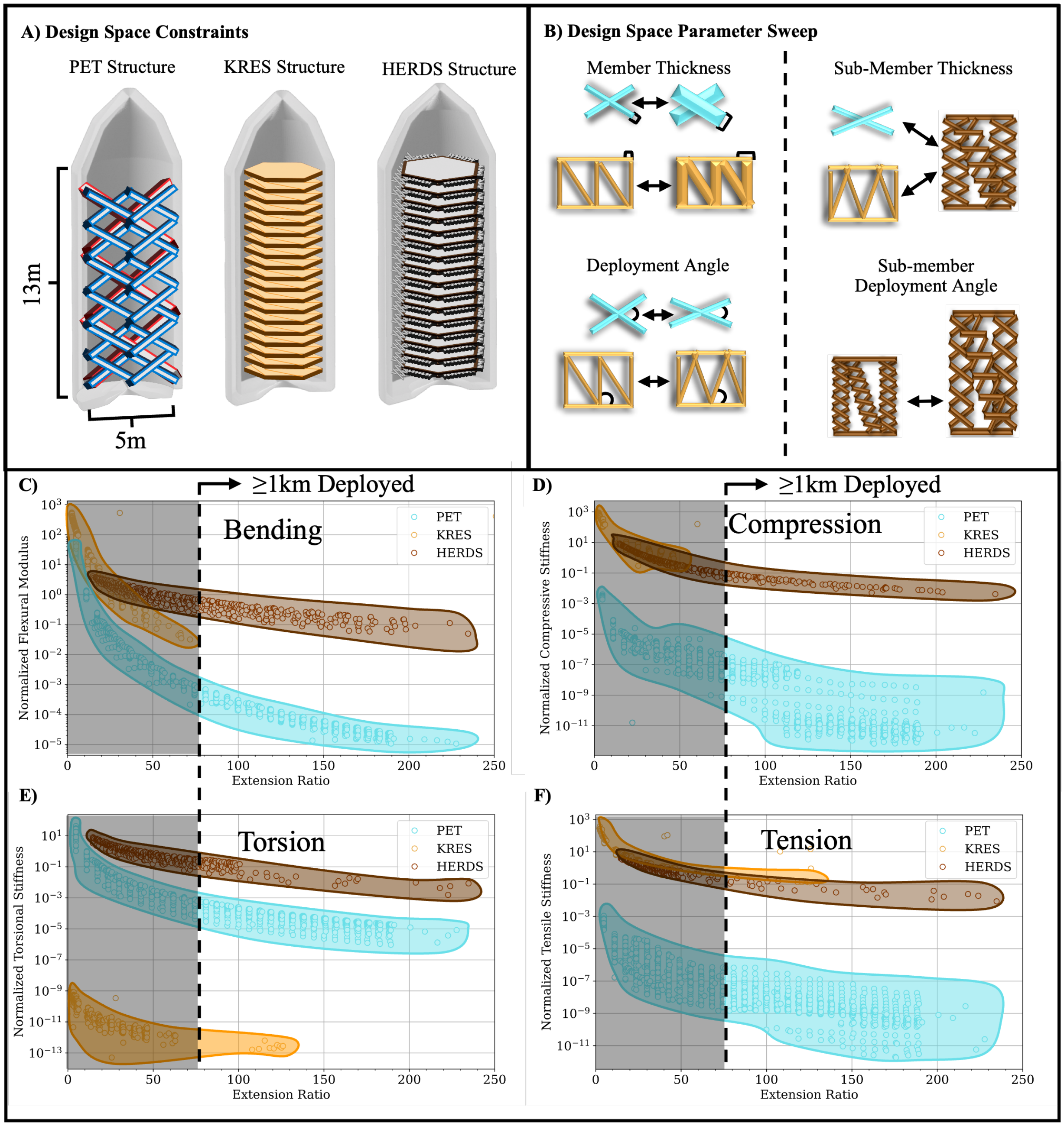

Figure 3.4: This figure presents a comparative analysis of the HERDS structure's performance in relation to its constituent elements, the PETs and Kresling, across different extension ratios and under various loads: **A) Design Space Constraints:** Details the stowed design space constraints for each of the members highlighting how each structure must fit in the fairing parameters close to Falcon 9 rocket. **B) Design Space Parameters:** Details the variable design parameters adjusted during the study, specifically for the Kresling and PET structures. These parameters include the PET aspect ratio, PET angle, Kresling angle, and Kresling width, all critical in defining the geometry and functionality of the deployable structures. **C) Bending Stiffness vs. Extension Ratio:** Illustrates the bending modulus performance of the PET, Kresling, and HERDS structures as a function of the extension ratio. **D) Compressive Stiffness vs. Extension Ratio:** Demonstrates the compressive stiffness of the structures across varying extension ratios. An accompanying simulation image reveals the potential buckling points in the PET substructures under compressive forces. **E) Torsional Stiffness vs. Extension Ratio:** This plot shows the results of the design's torsional stiffness as it relates to the extension ratio. At high extension ratios greater than 25x the HERDS outperforms the

scissor mechanisms. This physical model demonstrated cohesive reorientation of the many-component hierarchical structure without issues of jamming or mechanical frustration. The components included revolute joints with preloaded flexible tabs that automatically latched once each joint reached the fully deployed state, fixing its final position (details in SM. Figure 6).

Figure **??**.B shows structure deformation given global compressive loading. Despite being constructed from hand-assembled PLA plastic with suboptimal joint design and fabrication inconsistencies, this model could support a compressive load of 15 pounds and a bending load of 12 pounds without global failure. Based on the initial and final loaded structure beam angles, while this model shows some flexing in individual beams, most of the structure's deformation occurs at the Kresling joints that combine each PET beam. These stress concentrations qualitatively match simulation results. These observations indicate that future work should further optimize the latching joints to withstand greater loads with less strain. Enhanced joint tolerances, locking techniques, and material choices can further advance this design. Future work will seek to match the simulated results to the real data shown, with improvements towards modeling the joints, locking, and interfaces in the FEA simulation. Additional information about prototype fabrication and testing is added in SM Section 7 and SM Table 4.

Locking Considerations

The effectiveness of locking elements plays a critical role in determining the stiffness and structural integrity of a deployed mechanism. For a deployable system to function as a load-bearing structure, it must transition smoothly into its deployed configuration and maintain rigidity under load. While locking strategies are highly application-dependent and a full global locking architecture is beyond the scope of this paper, we conducted a preliminary investigation into this area as a proof of concept.

We designed and tested several 3D-printed locking mechanisms for a triangular scissor structure, including: pin and corner lock, pin lock, ramp and corner lock, ramp lock, no lock, glued pin, and fully rigid. Using three-point bend tests on beams with rigid and deployable configurations, we derived an effective stiffness for each substructure. As shown in Supplementary Figure 6, the top-performing locking designs achieved approximately 80% of the stiffness of a fully rigid connection. Notably, Figure **??**.B shows that the PET structure itself achieved a 71% improvement in bending stiffness over a standard solid beam, demonstrating the structural benefit of the substructure despite some compliance introduced by the locking elements. Although optimizing locking mechanisms was not a central focus of this work, these findings highlight their importance and inform future directions. Since many of our prototypes were fabricated from 3D-printed PLA, we also tested reinforcement strategies such as tensioned cables (Figure SM 5) to enhance structural performance. Locking and reinforcement strategies will be critical for maturing deployable mechanisms into reliable, load-bearing structures.

3.3 Conclusions

This work introduced Hierarchical Extending and Reorienting Deployable Structures (HERDS), a novel non-planar deployable mechanism composed of reorienting substructures. Through an extensive finite element design sweep, we demonstrated that HERDS outperforms its subcomponent mechanisms—the Kresling and PET structures—in flexural, torsional, compressive, and tensile stiffness at high extension ratios (above 25x). These improvements stem from HERDS' ability to tightly pack in the stowed state while increasing bending resistance upon deployment, a benefit derived from the reorientation and composition of its substructures.

Among the key findings, the Pop-Up Extending Truss (PET) plays a critical role by improving packing density when integrated with Kresling superstructures and contributing to a 71% improvement in flexural modulus over a solid beam of equal mass. Compared to standard scissor mechanisms, PETs achieved over 100% improvement in flexural modulus-to-mass ratio. However, at lower extension ratios (below 25x), traditional Kresling and PET mechanisms outperform HERDS due to the lower effective moment of inertia of reorienting small members.

We validated these trends with a 3D-printed HERDS prototype demonstrating smooth deployment at 50x expansion. Observations confirmed built-in redundancy: several members failed during repeated deployments without compromising overall function, suggesting inherent fault tolerance. However, critical challenges remain: the junctions between substructures are prone to stress concentration and require improved locking strategies to achieve load-bearing rigidity. Although preliminary locking mechanism tests yielded up to 80% stiffness compared to rigid connections, robust, reusable, and scalable locking remains an open area of development.

Fabrication and joint design present key limitations that need to be further explored, due to the complex boundary conditions, especially for flight-rated materials and environments. Current prototypes used PLA and simple mechanical joints; transitioning to high-performance composites and precision-engineered joints and locking will be necessary for aerospace deployment. This investigated the performance within volume-constrained packaging scenarios, such as rocket fairings, and validated the performance against the system's substructures. Future studies will benchmark HERDS directly against the large corpus of aerospace deployables, including rollable booms, coilable masts, and stacers.

This work investigates a new class of non-planar hierarchical deployable structures with scalable applications. These mechanisms hold promise for space-based infrastructure, such as kilometer-scale artificial gravity habitats or large antennas, and for terrestrial needs, such as lightweight, stowable towers for disaster response or remote communications. Future work will explore joint design, locking strategies, fundamental frequency analysis, and robustness compared to existing solutions to ensure that the new designs proposed meet the demands of real-world deployment and enable richer capabilities for Earth and beyond.

3.4 Methods

Extended details on PET, Kresling, and HERDS are provided in the Supplementary Information. This includes specific information about the geometry, the FEM simulations, the design sweeps, the fabrication of the prototype, and results from locking mechanism testing.

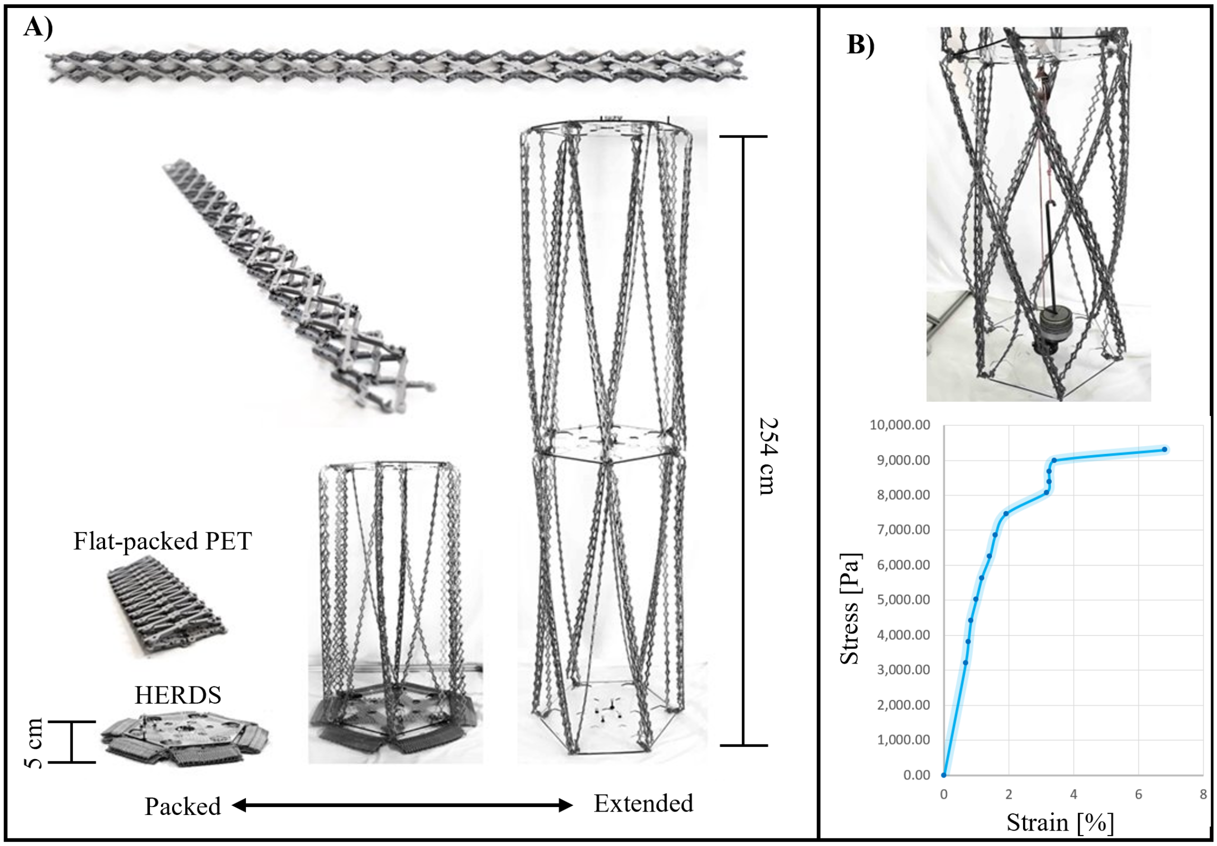

Figure 3.5: This figure shows the validation of a hierarchical design framework using a physical prototype: **A) Hardware Demonstration :** Showcases the sequential deployment process of both the PET and HERDS structures. It details three stages: from a completely flat-packed PET, indicative of its compact state, to the intermediate and fully extended forms, with the latter highlighting the extension capability, reaching a height of 244 cm from an initial compact height of just 6.3 cm. **B) Compressive Testing:** Presents a view of the HERDS under a compression test, leading to its faiure point, along with the corresponding stress-strain curve from the physical model testing. The curve displays the mechanical behavior of the HERDS, ending with a sharp increase in strain, which likely corresponds to the structural failure observed in the prototype.

Part I

Conclusions and Future Directions

Conclusions and Future Directions

here are my conclusions

Bibliography

This bibliography contains ?? references.

[1] Sourish Banerjee. “On the mechanical properties of hierarchical lattices”. en. In: *Mechanics of Materials* 72 (May 2014), pp. 19–32. ISSN: 0167-6636. DOI: 10.1016/j.mechmat.2014.01.009. URL: https://www.sciencedirect.com/science/article/pii/S0167663614000209 (visited on 12/07/2022).

[2] Jens Bauer, Lucas R. Meza, Tobias A. Schaedler, Ruth Schwaiger, Xiaoyu Zheng, and Lorenzo Valdevit. “Nanolattices: An Emerging Class of Mechanical Metamaterials”. en. In: *Advanced Materials* 29.40 (2017), p. 1701850. ISSN: 1521-4095. DOI: 10.1002/adma.201701850. URL: https://onlinelibrary.wiley.com/doi/abs/10.1002/adma.201701850 (visited on 02/05/2024).

[3] Michael A. Brown. “A deployable mast for solar sails in the range of 100–1000m”. en. In: *Advances in Space Research*. SOLAR SAILING: CONCEPTS, TECHNOLOGY, AND MISSIONS 48.11 (Dec. 2011), pp. 1747–1753. ISSN: 0273-1177. DOI: 10.1016/j.asr.2011.01.014. URL: https://www.sciencedirect.com/science/article/pii/S0273117711000615 (visited on 11/22/2022).

[4] David Cadogan and John Lin. “Inflatable solar array technology”. In: *37th Aerospace Sciences Meeting and Exhibit*. 1999, p. 1075. URL: https://doi.org/10.2514/6.1999-1075.

[5] Qiang Chen and Nicola M. Pugno. “Bio-mimetic mechanisms of natural hierarchical materials: A review”. en. In: *Journal of the Mechanical Behavior of Biomedical Materials*. Science and Engineering of Natural Materials: Merging Structure and Materials 19 (Mar. 2013), pp. 3–33. ISSN: 1751-6161. DOI: 10.1016/j.jmbbm.2012.10.012. URL: https://www.sciencedirect.com/science/article/pii/S1751616112002706 (visited on 12/07/2022).

[6] John Chilton. *Space Grid Structures (1st ed.)* Routledge., 1999. URL: https://doi.org/10.4324/9780080498188.

[7] Junwoo Choi, Dongkyu Lee, Kukha Hwang, and Byungkyu Kim. “Design, fabrication, and evaluation of a passive deployment mechanism for deployable space telescope”. In: *Advances in Mechanical Engineering* 11.5 (2019), p. 1687814019852258. URL: https://doi.org/10.1177/1687814019852258.

[8] ZhongYi Chu and YiAn Lei. “Design theory and dynamic analysis of a deployable boom”. en. In: *Mechanism and Machine Theory* 71 (Jan. 2014), pp. 126–141. ISSN: 0094-114X. DOI: 10.1016/j.mechmachtheory.2013.09.009. URL: https://

www.sciencedirect.com/science/article/pii/S0094114X13001857 (visited on 11/22/2022).

[9] Brett Cooper, Jonathan Black, Eric Swenson, and Richard Cobb. "Rigidizable inflatable get-away-special experiment (RIGEX) space flight data analysis". In: *50th AIAA/ASME/ASCE/AHS/ASC Structures, Structural Dynamics, and Materials Conference 17th AIAA/ASME/AHS Adaptive Structures Conference 11th AIAA No.* 2009, p. 2157. URL: https://doi.org/10.2514/6.2009-2157.

[10] Delin Cui, Shaoze Yan, Xiaosong Guo, and Fulei Chu. "An overview of dynamics modeling of inflatable solar array". In: *Energy Procedia* 14 (2012), pp. 1967–1972. URL: https://doi.org/10.1016/j.egypro.2011.12.1195.

[11] Y Cui and Y Tang. "The in-orbit core test of Shijian-20 satellite has been completed". In: *Space International* 7 (2020), pp. 38–41.

[12] NA Dollah, MR Saad, and A CheIdris. "Inflatable structure for aerospace application: Historical perspective and future outlook". In: *Journal of Fundamental and Applied Sciences* 9.3S (2017), pp. 317–334. URL: https://doi.org/10.4314/jfas.v9i3s.26.

[13] Giulia E Fenci and Neil GR Currie. "Deployable structures classification: A review". In: *International Journal of Space Structures* 32.2 (2017), pp. 112–130. DOI: 10.1177/0266351117711290. eprint: https://doi.org/10.1177/0266351117711290. URL: https://doi.org/10.1177/0266351117711290.

[14] Juan M. Fernandez. "Advanced Deployable Shell-Based Composite Booms for Small Satellite Structural Applications Including Solar Sails". In: NTRS Author Affiliations: NASA Langley Research Center NTRS Report/Patent Number: NF1676L-25486 NTRS Document ID: 20170001569 NTRS Research Center: Langley Research Center (LaRC). Kyoto, Jan. 2017. URL: https://ntrs.nasa.gov/citations/20170001569 (visited on 11/22/2022).

[15] Mitchell B. Fogelson, Sawyer Thomas, Giusy Falcone, Jeffrey I. Lipton, and Zachary Manchester. "High-Expansion-Ratio Deployable Space Structures for Long Duration Space Missions". In: *2024 IEEE Aerospace Conference*. 2024, pp. 1–10. DOI: 10.1109/AERO58975.2024.10521270. URL: https://ieeexplore.ieee.org/abstract/document/10521270.

[16] Peter Fratzl and Richard Weinkamer. "Nature's hierarchical materials". In: *Progress in Materials Science* 52.8 (Nov. 2007), pp. 1263–1334. ISSN: 0079-6425. DOI: 10.1016/j.pmatsci.2007.06.001. URL: https://www.sciencedirect.com/science/article/pii/S007964250700045X (visited on 02/05/2024).

[17] Ruben Gatt, Luke Mizzi, Joseph I. Azzopardi, Keith M. Azzopardi, Daphne Attard, Aaron Casha, Joseph Briffa, and Joseph N. Grima. "Hierarchical Auxetic Mechanical Metamaterials". en. In: *Scientific Reports* 5.1 (Feb. 2015), p. 8395. ISSN: 2045-2322. DOI: 10.1038/srep08395. URL: https://www.nature.com/articles/srep08395 (visited on 04/11/2024).

[18] Mark S Grahne and David P Cadogan. "Deployment control mechanisms and packaging methodologies for inflatable and membrane space structures". In: *Progress in*

Astronautics and Aeronautics. 191 (2001), pp. 417–431. URL: https://doi.org/10.2514/5.9781600866616.0417.0431.

[19] Fiona A. Harrison et al. "THE *NUCLEAR SPECTROSCOPIC TELESCOPE ARRAY* (*NuSTAR*) HIGH-ENERGY X-RAY MISSION". en. In: *The Astrophysical Journal* 770.2 (May 2013), p. 103. ISSN: 0004-637X, 1538-4357. DOI: 10.1088/0004-637X/770/2/103. URL: https://iopscience.iop.org/article/10.1088/0004-637X/770/2/103 (visited on 11/22/2022).

[20] ANSYS Inc. *ANSYS® APDL Academic Research Mechanical, Release 22 R2.*

[21] Alexander Kaszynski. *pyansys: Pythonic interface to MAPDL.* Version 0.60.3. Nov. 2021. DOI: 10.5281/zenodo.4009466. URL: https://doi.org/10.5281/zenodo.4009466.

[22] P Keith Kelly. "A scalable deployable high gain antenna-DaHGR". In: (2016). URL: https://digitalcommons.usu.edu/smallsat/2016/TS7Communication/6/.

[23] Tae-Hyun Kim, Jong-Eun Suh, and Jae-Hung Han. "Deployable truss structure with flat-form storability using scissor-like elements". en. In: *Mechanism and Machine Theory* 159 (May 2021), p. 104252. ISSN: 0094-114X. DOI: 10.1016/j.mechmachtheory.2021.104252. URL: https://www.sciencedirect.com/science/article/pii/S0094114X21000100 (visited on 11/17/2022).

[24] Takayuki Kitamura, Koichi Yamashiro, Akira Obata, and Michihiro Natori. "Development of a high stiffness extendible and retractable mast'HIMAT'for space applications". In: *31st structures, structural dynamics and materials conference.* 1990, p. 1054. URL: https://doi.org/10.2514/6.1990-1054.

[25] Y Kojima, T Tamura, Y Nozaki, and Y Onishi. "The development of high efficiency flexible solar array paddle of ADEOS-II". In: *Conference Record of the Twenty Fifth IEEE Photovoltaic Specialists Conference-1996.* IEEE. 1996, pp. 321–324. URL: https://ieeexplore.ieee.org/document/564010.

[26] Roderic Lakes. "Materials with structural hierarchy". en. In: *Nature* 361.6412 (Feb. 1993), pp. 511–515. ISSN: 0028-0836, 1476-4687. DOI: 10.1038/361511a0. URL: http://www.nature.com/articles/361511a0 (visited on 11/22/2022).

[27] Hai-Quan Li, Xiao-Feng Liu, Shao-Jing Guo, and Guo-Ping Cai. "Deployment dynamics and control of large-scale flexible solar array system with deployable mast". en. In: *Advances in Space Research* 58.7 (Oct. 2016), pp. 1288–1302. ISSN: 0273-1177. DOI: 10.1016/j.asr.2016.06.008. URL: https://www.sciencedirect.com/science/article/pii/S0273117716303064 (visited on 11/22/2022).

[28] "Lightweight Deployable Booms: Design, Manufacture, Verification, and Smart Materials Application". en. In: *55th International Astronautical Congress of the International Astronautical Federation, the International Academy of Astronautics, and the International Institute of Space Law.* Vancouver, British Columbia, Canada: American Institute of Aeronautics and Astronautics, Oct. 2004. DOI: 10.2514/6.IAC-04-I.4.10. URL: http://arc.aiaa.org/doi/10.2514/6.IAC-04-I.4.10 (visited on 11/22/2022).

[29] MC Lou and VA Feria. "Development of space inflatable/rigidizable structures technology". In: *IUTAM-IASS Symposium on Deployable Structures: Theory and Appli-*

cations: Proceedings of the IUTAM Symposium held in Cambridge, UK, 6–9 September 1998. Springer. 2000, pp. 251–260. URL: https://hdl.handle.net/2014/20321.

[30] Xiaofei Ma, Tuanjie Li, Jingya Ma, Zhiyi Wang, Chuang Shi, Shikun Zheng, Qifeng Cui, Xiao Li, Fan Liu, Hongwei Guo, et al. "Recent advances in space-deployable structures in China". In: *Engineering* 17 (2022), pp. 207–219. URL: https://doi.org/10.1016/j.eng.2022.04.013.

[31] Akira Meguro, Kyoji Shintate, Motofumi Usui, and Akio Tsujihata. "In-orbit deployment characteristics of large deployable antenna reflector onboard Engineering Test Satellite VIII". In: *Acta Astronautica* 65.9-10 (2009), pp. 1306–1316. URL: https://doi.org/10.1016/j.actaastro.2009.03.052.

[32] Martin M. Mikulas. "Truss Performance and Packaging Metrics". en. In: *AIP Conference Proceedings*. Vol. 813. Albuquerque, New Mexico (USA): AIP, 2006, pp. 1000–1009. DOI: 10.1063/1.2169281. URL: https://pubs.aip.org/aip/acp/article/813/1/1000-1009/813938 (visited on 01/27/2025).

[33] B. P. Nagaraj, R. Pandiyan, and Ashitava Ghosal. "Kinematics of pantograph masts". en. In: *Mechanism and Machine Theory* 44.4 (Apr. 2009), pp. 822–834. ISSN: 0094-114X. DOI: 10.1016/j.mechmachtheory.2008.04.004. URL: https://www.sciencedirect.com/science/article/pii/S0094114X08000876 (visited on 11/17/2022).

[34] J. Pérez-Valcárcel, M. Muñoz-Vidal, F. Suárez-Riestra, Isaac R. López-César, and M. J. Freire-Tellado. "A new system of deployable structures with reciprocal linkages for emergency buildings". en. In: *Journal of Building Engineering* 33 (Jan. 2021), p. 101609. ISSN: 2352-7102. DOI: 10.1016/j.jobe.2020.101609. URL: https://www.sciencedirect.com/science/article/pii/S2352710220306082 (visited on 11/22/2022).

[35] L. Puig, A. Barton, and N. Rando. "A review on large deployable structures for astrophysics missions". en. In: *Acta Astronautica* 67.1 (July 2010), pp. 12–26. ISSN: 0094-5765. DOI: 10.1016/j.actaastro.2010.02.021. URL: https://www.sciencedirect.com/science/article/pii/S0094576510000743 (visited on 11/22/2022).

[36] Joshua E. Salazar and Juan M. Fernandez. "Experimental Characterization of the Dimensional Stability of Deployable Composite Booms During Stowage". en. In: *AIAA Scitech 2021 Forum*. VIRTUAL EVENT: American Institute of Aeronautics and Astronautics, Jan. 2021. ISBN: 978-1-62410-609-5. DOI: 10.2514/6.2021-0195. URL: https://arc.aiaa.org/doi/10.2514/6.2021-0195 (visited on 11/22/2022).

[37] Tobias A. Schaedler and William B. Carter. "Architected Cellular Materials". In: *Annual Review of Materials Research* 46.1 (2016), pp. 187–210. DOI: 10.1146/annurev-matsci-070115-031624. URL: https://doi.org/10.1146/annurev-matsci-070115-031624 (visited on 02/02/2024).

[38] Mark Schenk, Andrew D Viquerat, Keith A Seffen, and Simon D Guest. "Review of inflatable booms for deployable space structures: packing and rigidization". In: *Journal of Spacecraft and Rockets* 51.3 (2014), pp. 762–778. URL: https://doi.org/10.2514/1.A32598.

[39] R. Schwaiger, L. R. Meza, and X. Li. "The extreme mechanics of micro- and nanoarchitected materials". en. In: *MRS Bulletin* 44.10 (Oct. 2019), pp. 758–765. ISSN: 0883-

7694, 1938-1425. DOI: 10.1557/mrs.2019.230. URL: https://www.cambridge.org/core/journals/mrs-bulletin/article/extreme-mechanics-of-micro-and-nanoarchitected-materials/25A7986D38FDEC8FC510F5EB07CD382F#ref15 (visited on 02/05/2024).

[40] Eugene R Schwanbeck. "Advanced Solar Arrays on the ISS". In: *Association of Space Explorers (ASE) Planetary Congress 2019*. JSC-E-DAA-TN74083. 2019. URL: https://ntrs.nasa.gov/citations/20190032191.

[41] Zheng Shi-kun, Ji You-zhi, Cui Zhao-yun, Fang Yong-gang, and Zhou Li-ping. "Design and analysis of HJ-1-C satellite SAR antenna". In: 3.3 (2014), pp. 266–273. URL: https://doi.org/10.3724/SP.J.1300.2014.14040.

[42] Jason Shore, Andrew Viquerat, Guy Richardson, and Guglielmo Aglietti. "Effects of the root condition on the stiffness of a deployable boom structure". en. In: *AIAA Scitech 2021 Forum*. VIRTUAL EVENT: American Institute of Aeronautics and Astronautics, Jan. 2021. ISBN: 978-1-62410-609-5. DOI: 10.2514/6.2021-0297. URL: https://arc.aiaa.org/doi/10.2514/6.2021-0297 (visited on 11/22/2022).

[43] Tarah N. Sullivan, Bin Wang, Horacio D. Espinosa, and Marc A. Meyers. "Extreme lightweight structures: avian feathers and bones". In: *Materials Today* 20.7 (Sept. 2017), pp. 377–391. ISSN: 1369-7021. DOI: 10.1016/j.mattod.2017.02.004. URL: https://www.sciencedirect.com/science/article/pii/S136970211730072X (visited on 02/01/2024).

[44] D Tian, H Gao, L Jin, R Liu, X Ma, X Fan, and Z Guo. "Research status and prospect of modular space deployable and foldable mechanism". In: *China Space Science and Technology* 41.4 (2021), pp. 16–31. URL: https://doi.org/10.16708/j.cnki.1000-758X.2021.0047.

[45] Gunnar Tibert and Sergio Pellegrino. "Deployable Tensegrity Masts". In: *44th AIAA/ASME/ASCE/AHS/ASC Structures, Structural Dynamics, and Materials Conference*. American Institute of Aeronautics and Astronautics, 2012. DOI: 10.2514/6.2003-1978. URL: https://arc.aiaa.org/doi/abs/10.2514/6.2003-1978 (visited on 11/22/2022).

[46] Jeffrey Umland and Howard Eisen. "SRTM on-orbit structural dynamics". In: *19th AIAA Applied Aerodynamics Conference*. DOI: 10.2514/6.2001-1588. eprint: https://arc.aiaa.org/doi/pdf/10.2514/6.2001-1588. URL: https://arc.aiaa.org/doi/abs/10.2514/6.2001-1588.

[47] Bing Wang, Juncheng Zhu, Shuncong Zhong, Wei Liang, and Chenglong Guan. "Space deployable mechanics: A review of structures and smart driving". In: *Materials Design* 237 (2024), p. 112557. ISSN: 0264-1275. DOI: https://doi.org/10.1016/j.matdes.2023.112557. URL: https://www.sciencedirect.com/science/article/pii/S0264127523009735.

[48] Sicong Wang, Mark Schenk, Shengyuan Jiang, and Andrew Viquerat. "Blossoming analysis of composite deployable booms". en. In: *Thin-Walled Structures* 157 (Dec. 2020), p. 107098. ISSN: 0263-8231. DOI: 10.1016/j.tws.2020.107098. URL: https://www.sciencedirect.com/science/article/pii/S0263823120309721 (visited on 11/22/2022).

[49] Kun Xu, Long Li, Shaoping Bai, Qiaolong Yang, and Xilun Ding. "Design and analysis of a metamorphic mechanism cell for multistage orderly deployable/retractable mechanism". In: *Mechanism and Machine Theory* 111 (May 2017), pp. 85–98. ISSN: 0094-114X. DOI: 10.1016/j.mechmachtheory.2017.01.016. URL: https://www.sciencedirect.com/science/article/pii/S0094114X16304347 (visited on 01/04/2024).

[50] Zhihui Xue, Jinguo Liu, Chenchen Wu, and Yuchuang Tong. "Review of in-space assembly technologies". In: *Chinese Journal of Aeronautics* 34.11 (Nov. 2021), pp. 21–47. ISSN: 1000-9361. DOI: 10.1016/j.cja.2020.09.043. URL: https://www.sciencedirect.com/science/article/pii/S1000936120304854 (visited on 02/10/2025).

[51] Hui Yang, Shuoshuo Fan, Yan Wang, and Chuang Shi. "Novel Four-Cell Lenticular Honeycomb Deployable Boom with Enhanced Stiffness". en. In: *Materials* 15.1 (Jan. 2022), p. 306. ISSN: 1996-1944. DOI: 10.3390/ma15010306. URL: https://www.mdpi.com/1996-1944/15/1/306 (visited on 11/22/2022).

[52] Hui Yang, Lian Liu, Hongwei Guo, Fengshuai Lu, and Yongbin Liu. "Wrapping dynamic analysis and optimization of deployable composite triangular rollable and collapsible booms". en. In: *Structural and Multidisciplinary Optimization* 59.4 (Apr. 2019), pp. 1371–1383. ISSN: 1615-1488. DOI: 10.1007/s00158-018-2118-9. URL: https://doi.org/10.1007/s00158-018-2118-9 (visited on 11/22/2022).

[53] Z. You and S. Pellegrino. "Cable-stiffened pantographic deployable structures. I - Triangular mast". en. In: *AIAA Journal* 34.4 (Apr. 1996), pp. 813–820. ISSN: 0001-1452, 1533-385X. DOI: 10.2514/3.13144. URL: https://arc.aiaa.org/doi/10.2514/3.13144 (visited on 11/22/2022).

[54] Zhong You and Nicholas Cole. "Self-Locking Bi-Stable Deployable Booms". en. In: *47th AIAA/ASME/ASCE/AHS/ASC Structures, Structural Dynamics, and Materials Conference
 14th AIAA/ASME/AHS Adaptive Structures Conference
 7th*. Newport, Rhode Island: American Institute of Aeronautics and Astronautics, May 2006. ISBN: 978-1-62410-040-6. DOI: 10.2514/6.2006-1685. URL: http://arc.aiaa.org/doi/abs/10.2514/6.2006-1685 (visited on 11/22/2022).

[55] Xiangjie Yu, Bindi You, Xiaomeng Liu, and Qian Cao. "Nonlinear Dynamics Investigation of Variable Cross-Sectional Solar-Sail Masts". In: *Journal of Spacecraft and Rockets* 58.4 (2021), pp. 936–946. ISSN: 0022-4650. DOI: https://doi.org/10.2514/1.A34925. URL: https://doi.org/10.2514/1.A34925 (visited on 11/22/2022).

[56] LI Yuanyuan, LI Meng, LIU Yufei, GENG Xinyu, and CUI Chengbo. "Parameter optimization for torsion spring of deployable solar array system with multiple clearance joints considering rigid–flexible coupling dynamics". In: *Chinese Journal of Aeronautics* 35.3 (2022), pp. 509–524. URL: https://doi.org/10.1016/j.cja.2021.03.033.

[57] Zirui Zhai, Yong Wang, and Hanqing Jiang. "Origami-inspired, on-demand deployable and collapsible mechanical metamaterials with tunable stiffness". In: *Proceedings of the National Academy of Sciences* 115.9 (Feb. 2018), pp. 2032–2037. DOI: 10.1073/pnas.1720171115. URL: https://www.pnas.org/doi/full/10.1073/pnas.1720171115 (visited on 08/13/2024).

[58] ZQ Zhou, YM Wu, J Wang, Y Liu, Z Yan, and C Huang. “Development and trend of circular solar array”. In: *Spacecraft Engineering* 24.06 (2015), pp. 116–122.